# Mechanical Properties of Ultrananocrystalline Diamond Thin Films for MEMS Applications

H.D. Espinosa[1], B. Peng[1], K.-H. Kim[1], B.C. Prorok[2], N. Moldovan[3], X.C. Xiao[3], J.E. Gerbi[3], J. Birrell[3], O. Auciello[3], J.A. Carlisle[3], D.M. Gruen[3], and D.C. Mancini[3]

[1] Department of Mechanical Engineering, Northwestern University
Evanston, IL 60208-3111, USA
[2] Materials Research and Education Center, Auburn University, Auburn, AL 36849-5341, USA
[3] Materials Science and Experimental Facilities Divisions, Argonne National Laboratory
Argonne, IL 60439, USA

## ABSTRACT

Microcantilever deflection and the membrane deflection experiment (MDE) were used to examine the elastic and fracture properties of ultrananocrystalline diamond (UNCD) thin films in relation to their application to microelectromechanical systems (MEMS). Freestanding microcantilevers and membranes were fabricated using standard MEMS fabrication techniques adapted to our UNCD film technology. Elastic moduli measured by both methods described above are in agreement, with the values being in the range 930 and 970 GPa with both techniques showing good reproducibility. The MDE test showed fracture strength to vary from 3.95 to 5.03 GPa when seeding was performed with ultrasonic agitation of nanosized particles.

## INTRODUCTION

Carbon in its various forms, specifically diamond, may become a key material for the manufacturing of MEMS/NEMS devices in the 21st Century. The new ultrananocrystalline diamond (UNCD) films developed at Argonne National Laboratory [1] may provide the basis for revolutionary microelectromechanical systems (MEMS) and nanoelectromechanical systems (NEMS). The UNCD films are grown using a microwave plasma chemical vapor deposition technique involving a novel $CH_4$/Ar chemistry. The process yields films with extremely small grain size (2-5 nm), significantly smaller than nanocrystalline diamond films (30-100 nm grain size) produced by the conventional $CH_4$/H chemistry [2,3]. The UNCD films posses many of the outstanding physical properties of diamond, i.e., they exhibit exceptional hardness, extremely low friction coefficient and wear, high thermal and electrical conductivity, the latter when doped with nitrogen [4]. Preliminary results have shown that this unique microstructure results in outstanding mechanical properties (~ 97 GPa hardness and 967 GPa Young's modulus that are similar to single crystal diamond [5]), unique tribological properties (coefficient of friction of the order of ~0.02-0.03, [6]), and field-induced electron emission (threshold voltage 2-3 V/µm, [7]).

Preliminary work by investigators at Argonne has demonstrated the feasibility of fabricating 2-D and 3-D MEMS components that can be the basis for the fabrication of complete MEMS / NEMS devices [8-10]. Components such as cantilevers and multi-level devices such as microturbines have already been produced. These preliminary exercises are promising steps toward full-scale application of UNCD components in functional MEMS devices. However, before full-scale integration can occur, several intrinsic material properties, such as elastic modulus, plasticity and fracture of undoped and doped UNCD must be well characterized to fully exploit the potential of this material. In this paper, we use micro-cantilever deflection and the membrane deflection experiment [11] techniques to gain a better understanding of the elastic modulus and fracture strength for UNCD thin films. We have taken special care to design different specimen characteristics for each technique in an attempt to minimize effects in each that hinder accurate property measurements.

## EXPERIMENTAL PROCEDURE

Two types of specimens were used in this study. Both consist of freestanding, thin-films of UNCD with thickness ranging between 0.55 to 0.65 µm. The films are grown directly onto a Si substrate and specimen structures were microfabricated using standard techniques as described in Moldovan et al. [10]. Two structures were constructed, freestanding cantilevers and fixed-fixed membranes. Figure 1 is an SEM image and 3D schematic view of the cantilever structure. The dimensions of the cantilever are defined on the figure with $t$ as the thickness, $b$ as the width (20 µm for all cantilevers), and $l$ as the cantilever length (200 µm) at the point of contact during deflection. The structure of the cantilevers contained an etching undercut that resulted in the specimens having a "T" shape. This is accounted for in the data reduction procedure and is described later. The second type of specimen consists of specially designed double-dog-bone, freestanding membranes as shown later Figure 4. The specimens are designed to minimize stress concentrations and boundary bending effects. When vertically deflected, direct tension is produced in the gauge regions resulting in uniform specimen stressing. Further details are given in Espinosa et al. [11]. Specimens with gauge lengths of 300 µm and gauge widths of ~ 13.5 µm were tested. Both structures were probed with a nanoindenter to obtain high-resolution load-deflection signatures.

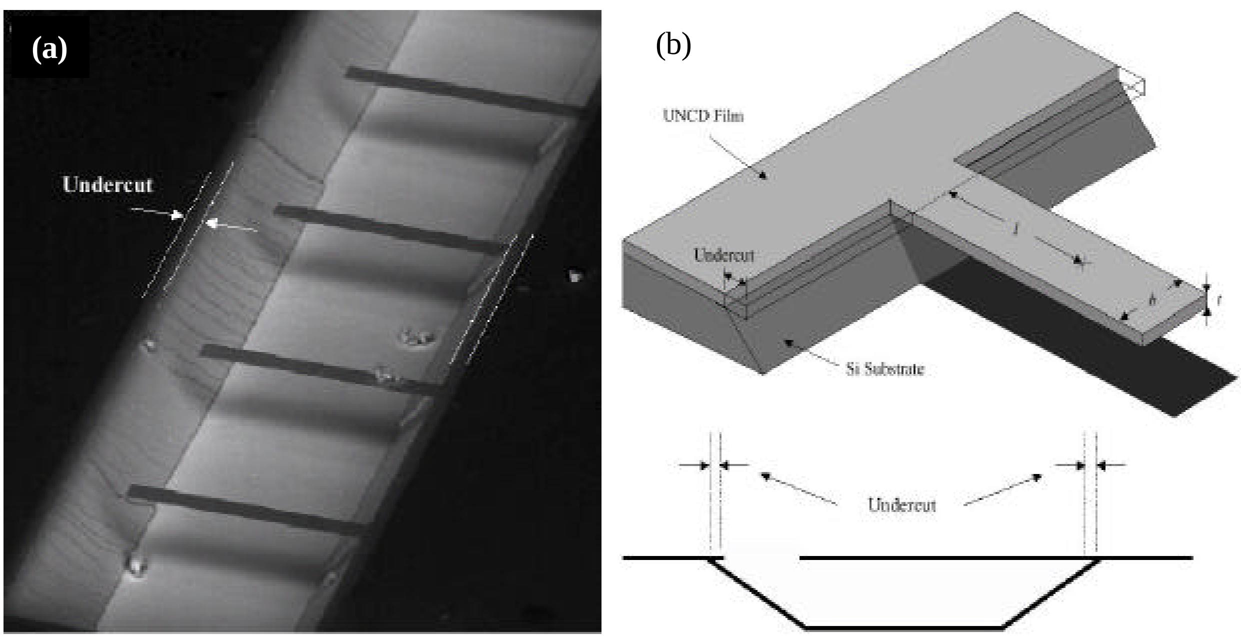


**Figure 1.** SEM image (a) and 3D schematic (b) of the freestanding UNCD cantilever structures. The figure illustrates an undercut resulting in a "T" shape. Parameters are defined in the text.

## RESULTS AND DISCUSSION

In order to test the load resolution of the nanoindenter a deflection test was performed on a single crystal (110) Si AFM tapping-mode tip, a material for which the elastic properties are well characterized; i.e., $E_{[111]}$ = 185 GPa, $E_{[110]}$ = 170 GPa and $E_{[100]}$ = 130 GPa [12]. Figure 2 shows optical images of the top- and bottom-view of the tip architecture illustrating a "T" shape. Dimensions of the tip where $b$ = 46.62 µm, $b_2$ = 197.93 µm, $t$ = 4.1 µm, $l$ = 100 µm, $l_u$ = 12 µm, and the taper around the top edge is 5.0 µm in width and 100 nm deep. Simulations were performed with these dimensions and the equivalent length, $l_{eq}$, was found to be 82.58 µm. Figure 2 shows the load-deflection curve for a cantilever test length of 80 µm. The stiffness, $k$, for different tests was found to vary between 2.58 x$10^{-4}$ to 2.61 x$10^{-4}$ mN/nm which corresponds to a modulus of 166 to 168 GPa, using the equation $k = Ebt^3/4l^3(1-v^2)$ using $v$ = 0.27, close to that of the [110] direction for Si, 170 GPa.

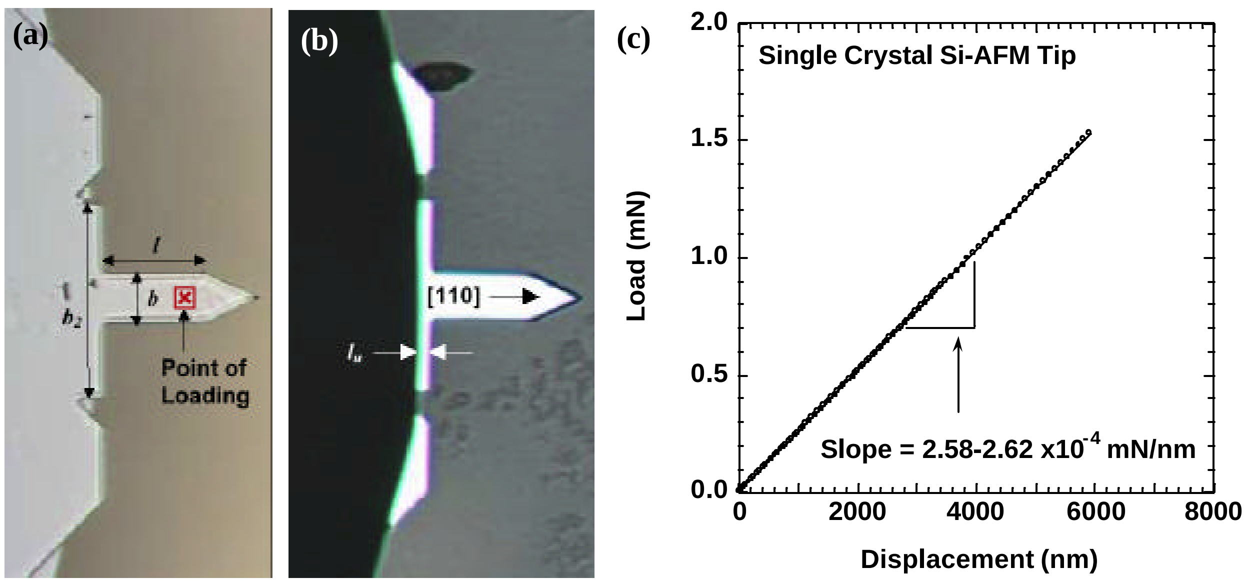


**Figure 2.** Optical images of (a) the top-view and (b) the bottom view of a silicon AFM tapping-mode tip. Undercut length is labeled as $l_u$. Load-displacement curve for the AFM tip (c).

Deflection of the UNCD cantilevers was accomplished by applying a concentrated load with a nanoindenter. Figure 3 (a) shows the load-deflection response of a typical cantilever with a length of 80 µm. The sudden increase in load at the beginning on the test in Fig. 3 (a) is believed to result from mechanisms involved in the nanoindenter tip contacting the cantilever surface. The slope of the linear region in Figure 3 (a) represents the elastic stiffness, $k$, of the UNCD cantilever. Using the parameters of $l$ = 80 µm, $l_u$ = 15.32 µm (measured), $k$ = 1.7x$10^{-6}$ mN/nm, $t$ = 0.6305 µm, and $b$ = 20 µm for the cantilever, simulations give an equivalent length of 88.2 µm and corresponding elastic modulus of 937 GPa. This value is higher than that measured by nanoindentation on UNCD that yielded an average value of 886 GPa [5]. Results of deflection for several other cantilevers, given later in Table 2, show elastic modulus to vary from 916-959. This scatter is the result of experimental errors associated to small inaccuracies in measuring film thickness and load with the nanoindenter. Tests were also performed on a single cantilever with load applied at different lengths, 60, 80, 100 and 120 µm, Figure 3 (b). The stiffness increased proportionally as the cantilever length decreased with measured elastic moduli of 937, 938, 957 and 958 GPa were obtained for cantilever lengths of 60, 80, 100, and 120 µm respectively.

An important aspect of the UNCD specimens used in the MDE measurements was that each specimen bowed outward, out of the wafer plane. This is believed to result from the difference in thermal expansion coefficients of Si and diamond, $\alpha_{Si} = 2.5x10^{-6}/°K$ and $\alpha_{Diamond} = 1.5x10^{-6}/°K$, and was characterized by interferometry. Figure 4 (a), shows the typical image obtained from the interferometer and the as generated x-z profile. The height above the plane of the wafer, $D_c$, is determined as well as the actual length of the curved membrane, which is used to determine the deflection downward such that the membrane becomes flattened out and uniform straining of the material begins, $D_s$. Figure 4 (b) shows different time intervals during a typical test with corresponding points on the load-deflection signature. Uniform stretching of the membrane begins at point 3.

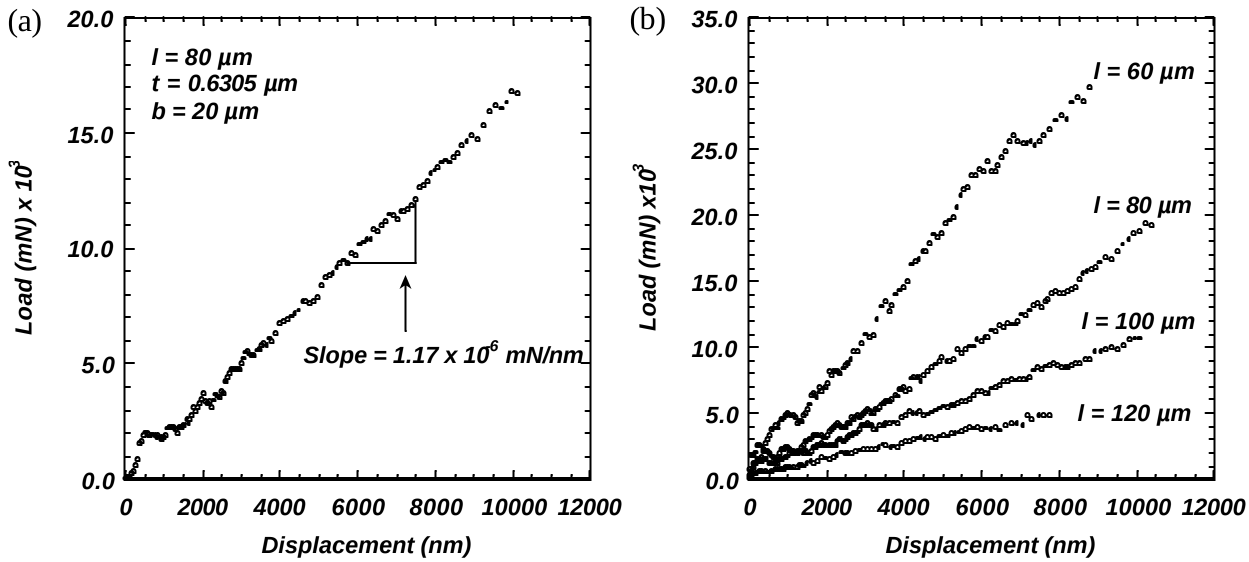


**Figure 3.** Load-deflection curve for an 80 µm-long cantilever (a) and comparing load-displacement for a single cantilever with load applied at lengths of 60, 80, 100 and 120 µm (b).

The stress-strain behavior can be obtained through converting the vertical nanoindenter load into the in-plane membrane load and then dividing by the cross-sectional area to obtain stress while using the interferometric images to obtain the strain, see Espinosa et al. for further details [11]. The stress-strain behavior is shown in Figure 5 (a). As mentioned above, the curve begins at a deflection where the membrane becomes stressed in pure tension, point 3 in Figure 4 (b). The slope of the plot represents the elastic modulus (948 GPa). Table 2 lists the elastic modulus and fracture stress of four identically shaped membranes. Modulus varied from 930 to 970 GPa and agrees well with the values obtained by micro-cantilever deflection. Failure stress varied in a statistical manner. Figure 5 (a) shows failure for UNCD samples occurring at 5.03 GPa, which compares very favorably with respect to fracture strengths of other materials (see Table 1). Table 2 compares the mechanical properties of UNCD specimens obtained using both testing techniques described here.

**Table 1.** Fracture Strengths of Other Hard Materials. (DLC=Diamond-Like Carbon)

| **Material** | **E (GPa)** | **$\sigma_f$ (GPa)** | **Material** | **E (GPa)** | **$\sigma_f$ (GPa)** |
|---|---|---|---|---|---|
| **Si** [13] | 150 | 0.30 | **$Si_3N_4$** [15,16] | 254 | 6.41 |
| **Poly-Si** [14] | 158 | 1.56 | **SiC** [17,18] | 373 | 1.44 |
| **UNCD** | 967 [5] | 5.03 [this work] | **DLC** [19] | 800 | 0.7 |

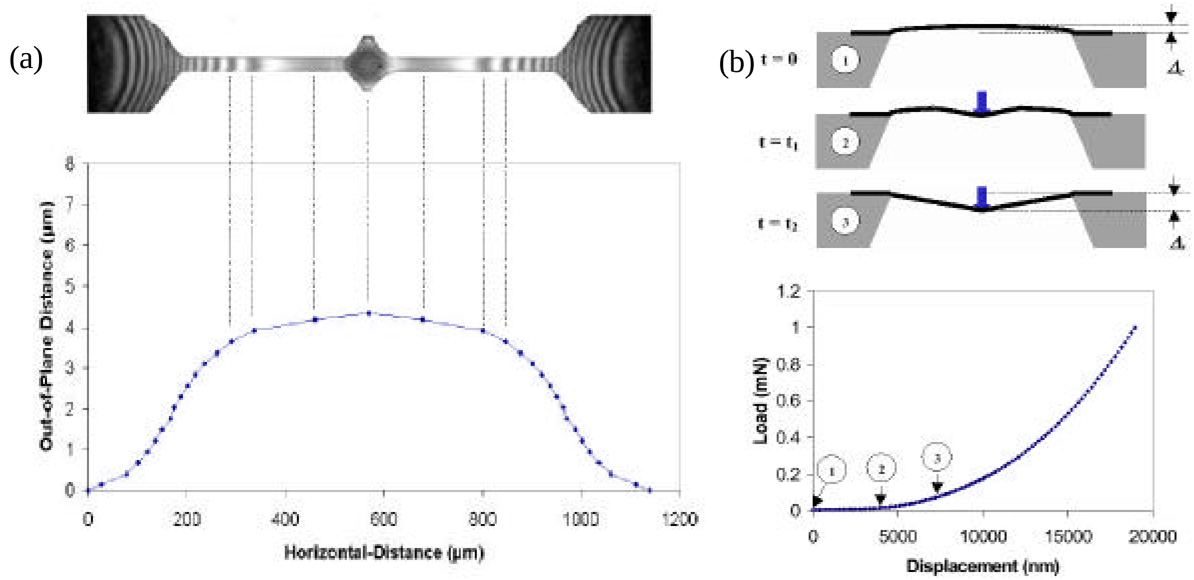


**Figure 4.** Interferometric characterization showing the out-of-plane bulging of the UNCD membranes (a) and its consequences in the MDE test (b) at three different time intervals.

In all specimens tested using the MDE method, failure occurred in the gauged region. This is illustrated in Figure 5 (b). In this SEM image, two tested membranes are shown. The upper sample has failed on the right-hand gauge while the bottom sample has failed simultaneously in both gauged regions. These images provide confidence that the controlling factors in the membrane behavior were confined to the gauged region.

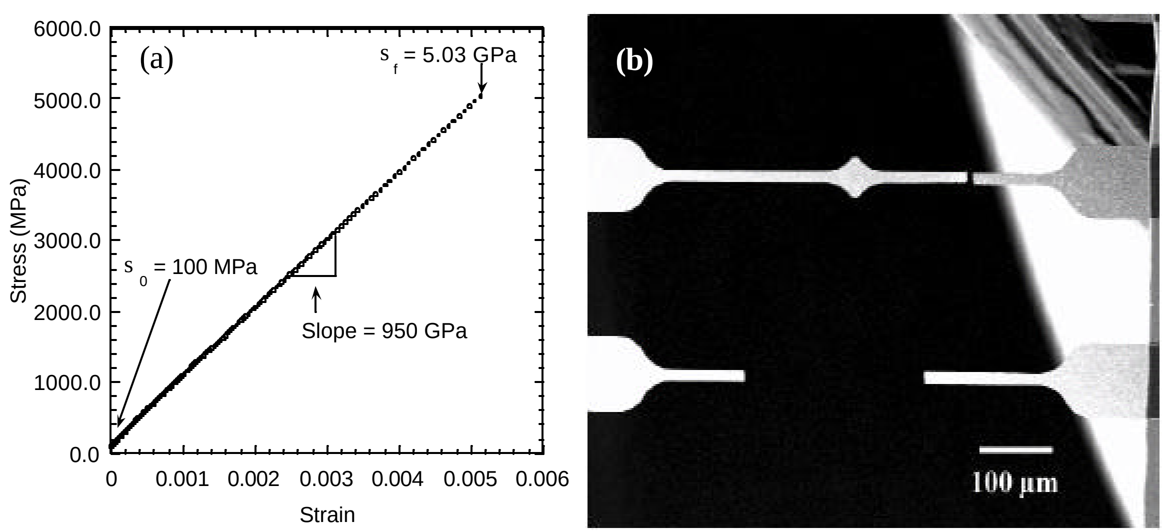


**Figure 1.** Stress-strain curve exhibited by the typical UNCD sample in the MDE test (a). Part (b) is an SEM image of two MDE Specimens illustrating that failure occurs in the gauged region.

**Table 2.** Comparison of Testing Techniques

| | Elastic Modulus (GPa) | Fracture Stress (GPa) |
|---|---|---|
| **Cantilever Deflection** | 916 to 959 | --------------- |
| **MDE – Microsized Seeding** | 930 to 970 | 0.89 to 2.42 |
| **MDE – Nanosized Seeding** | 945 to 963 | 3.95 to 5.03 |

## CONCLUSIONS

In this work, micro-cantilever deflection and membrane deflection techniques were used to determine the elastic modulus and fracture strength of ultrananocrystalline diamond (UNCD) thin films. Values of modulus ranging from 916 to 959 GPa were measured with the cantilever deflection technique. Characterization of the UNCD films by the membrane deflection experiment yielded elastic modulus values of 930-970 GPa. Fracture strength was found to be in the range of 5.05 GPa, when wafer seeding was performed with ultrasonic agitation with nanoscale particles, resulting in films with practically no defects. Both techniques were shown to yield repeatable and comparable results. The mechanical properties of UNCD films established in this work indicate that UNCD films can perform very well in MEMS devices.

## ACKNOWLEDGMENTS

This work was sponsored by the National Science Foundation under Career Award No. CMS-9624364 and the ONR-Young Investigator Program, Award No. N00014-97-1-0550.

## REFERENCES

1. D.M. Gruen, *Annu. Rev. Mater. Sci.* **29**, 211 (1999).
2. D.M. Gruen, S. Liu, A.R. Krauss, J. Luo, and X. Pan, *Appl. Phys. Lett.* **64**, 1502 (1994).
3. D.M. Gruen, S. Liu, A.R. Krauss, and X. Pan, *J. Appl. Phys.* **75**, 1758 (1994).
4. B. Bhattacharyya, O. Auciello, J. Birrell, J.A. Carlisle, L.A. Curtiss, A.N. Goyette, D.M. Gruen, A.R. Krauss, A. Sumant, and P. Zapol, *Appl. Phys. Lett.* **79**, 1441 (2001).
5. A.V. Sumant, O. Auciello, A.R. Krauss, D.M. Gruen, D. Ersoy, J. Tucek, A. Jayatissa, E. Stach, N. Moldovan, D. Mancini, H.G. Busmann, and E.M. Meyer, (2000), *Mat. Res. Soc. Symp. Proc.*, **657** (2000).
6. A. Erdemir, G.R. Fenske, A.R. Krauss, D.M. Gruen, T. McCauley, and R.T. Csencsits, *Surf. Coat. Technol.* **120-121**, 565 (1999).
7. A.R. Krauss, O. Auciello, M.Q. Ding, D.M. Gruen, Y. Huang, V.V. Zhirnov, E.I. Givargizov, A. Breskin, R. Chechen, E. Shefer, V. Konov, S. Pimenov, A. Karabutov, A. Rakhimov, and N. Suetin, *J. Appl. Phys.* **89**, 2958 (1999).
8. O. Auciello, A.R. Krauss, D.M. Gruen, H.G. Busmann, E.M. Meyer, J. Tucek, A. Sumant, A. Jayatissa, N. Moldovan, D. Mancini, and M.N. Gardos, *Mater. Res. Soc. Symp. Proc.* **605**, 78 (2000).
9. A.R. Krauss, O. Auciello, D.M. Gruen, A. Jayatissa, A. Sumant, J. Tucek, D. Mancini, N. Moldovan, A. Erdemir, D. Ersoy, M.N. Gardos, H.G. Busmann, E.M. Meyer, and M.Q. Ding, *Diam. Relat. Mater.* **10**, 1952 (2001).
10. N. Moldovan, A. Auciello, A. Sumant, J.A., Carlisle, R. Divan, D.M. Gruen, A.R. Krauss, D.C. Mancini, A. Jayatissa, and J. Tucek, *Proc. of SPIE* **4557**, 288 (2001).
11. H.D. Espinosa, B.C. Prorok, and M. Fischer, *J. Mech. Phys. Sol.* **51**, 67 (2003).
12. Y.A. Burenkov and S.P Nikanorov, *Sov. Phys.-Solid State* **16**, 963 (1974).
13. K.E. Peterson, *Proc. IEEE* **70**, 5 (1982).
14. W.N. Sharpe, Jr., K. Jackson, G. Coles and D.A. LaVan, *ASME Symp. On MEMS* **2** (2000).
15. G. Coles, W.N. Sharpe, Jr., and R.L. Edwards, *Proc. of MEMS: Soc. Exp. Mech.*, 1 (2001).
16. H. Kawaoka, T. Adachi, T. Sekino, L. Gao, and K. Niihara, *J. Mater. Res.* **16** (2001).
17. K. Lohner, K. Chen, A. Ayon and S. Spearing, *Mat. Res. Soc. Symp. Proc.* **546**, 85 (1999).
18. K. Lohner, K. Chen, A. Ayon and S.M. Spearing, *Mat. Res. Soc. Symp. Proc.* **546**, (1999).
19. S. Christiansen, M. Albrecht, and H.P. Strunk, *J. Mater. Res.* **11**, 8 (1996).